

# A Normalized SVD based Image Watermarking with an Enhanced Robustness and Imperceptibility

R. Surya Prakasa Rao<sup>1</sup>, Prof. P. Rajesh Kumar<sup>2</sup>

<sup>1</sup>Dept., of ECE, AU College of Engineering, Visakhapatnam, India.

<sup>2</sup>Dept., of ECE, AU College of Engineering, Visakhapatnam, India.  
reddisuryaprakash2014@gmail.com, rajeshauce@gmail.com

**Abstract:** Digital Image watermarking is one of the most active and challenging subjects in the information hiding research because it is an efficient solution to protect the copyright of the digital media. This paper proposes a new robust watermarking approach based on the selection of singular features of host image into which the watermark has to embed. The host image initially subjected to a normalization process to find the invariant features and then the obtained invariant features are subjected to Integer Wavelet Transform (IWT) followed by Normalized Singular value Decomposition (NSVD). NSVD normalizes the singular values of invariant sub bands which can effectively resist the attacks. Genetic Algorithm (GA) is used to normalize the singular values. After, the obtained normalized singular values are modified by adding the singular values of watermark image. At the embedding phase, Particle Swarm Optimization (PSO) was used to optimize watermarking constant. Numerous experiments are conducted over the proposed approach to evaluate the performance. The obtained experimental results demonstrates that the proposed approach is superior compared to conventional approaches and is able to provide efficient resistance over Gaussian noise, salt & pepper noise, median filtering, cropping, rotation, contrast enhancement, scaling and Histogram Equalization attacks.

**Index Terms:** Digital image watermarking, IWT, SVD, GA, PSO, PSNR, NC, SSIM.

## I. INTRODUCTION

Digital Image Watermarking [1, 2] is the process of insertion of image watermark in media content and its extraction, if required, for authentication or ownership verification of media content. A digital image watermark is a piece of information that is hidden directly in media content, in such a way that it is imperceptible to a human observer [3]. Different types of watermarking methods for digital contents have been developed that are classified into different categories depending upon the use and the requirement of information required for the extraction/detection of watermark. To check the authenticity of a digital content fragile watermarking is used while, for the purpose of copyright protection, robust watermarking is utilized. This classification is application-dependent. Based on the information required for the extraction/detection process watermarking schemes can be classified into blind, semi-blind, and non-blind categories. Also, one more categorization is possible depending upon the domain of embedding of watermark: spatial and frequency. A detailed review of watermarking schemes can be found in [4, 5]. In digital image watermarking, there will be a common problem rises at embedding phase. i.e., the optimization of embedding constant. This constant varies from image to image and also varies based on environments. Hence there is a need to optimize embedding constant such that the watermarked image must be robust and imperceptible to any type of environments. Generally, the artificial intelligence techniques such as Genetic algorithm (GA), Particle swarm optimization (PSO), Ant colony optimization (ACO) etc., techniques will be used for optimization purposes. In [6], a novel watermarking approach was proposed by combining the both GA and PSO to obtain an improved performance in watermarking criterion. However, [6] decomposes the image through the most popular Discrete wavelet transform (DWT) which is having main problem of information loss. Due to the down sampling process in DWT, the extracted watermark and also the host image can't recover entire information. Thus, the quality of the watermark will be reduced. In [7], a block based watermarking is proposed based on Discrete Wavelet Transform (DWT) and Singular Value decomposition (SVD). Initially, the host image was divided into the blocks of size 8X8 and then processed for DWT. From the obtained sub bands, the approximation band was subjected to SVD. Similarly all blocks are processed and the largest singular value is selected for embedding. However, it is observed that it is not robust for some types of attacks such as image rotation and image flipping. As the largest singular values from each block of the image have a different tolerance limit of modification to embed the watermark, it results in some visible distortions in the watermarked image with single scaling factor. In this paper, a new image watermarking approach is proposed by considering the both GA and PSO as an optimization techniques. This paper focuses towards the enhancement of robustness and also the imperceptibility. This approach incorporates the host image normalization and then processes for portioning into blocks to resist rotation and scaling attacks. Then IWT is applied on every block and the obtained approximation

band is subjected to normalized SVD. Here the normalized SVD is an extended version of SVD which normalizes the singular values through a constant. Then the obtained normalized singular values are processed for embedding. In this paper, the optimization problem is solved through Particle Swarm Optimization (PSO) and Genetic Algorithm (GA). The SVD optimization is carried out through GA and the optimization of embedding constant is carried out through PSO. The proposed approach is applied on various images and the performance was evaluated for various types of attacks. The rest of the paper is organized as follows: Section II illustrates the details of related work. Section III provides a review about the preliminary concepts used in this paper. Section IV illustrates the details of conventional approach completely. The complete details of proposed approach is given in section V. Section VI illustrates performance evaluation details and finally section VII concludes the paper.

## II. RELATED WORK

In a robust image watermarking scheme, a trade-off always exists among the two conflicting objectives, imperceptibility and robustness. So, the main goal of a robust image watermarking scheme is to produce the watermarked image with low quality degradation and high robustness. Therefore, in order to improve these objectives, researchers have proposed several watermarking schemes implemented in spatial as well as transformed domain that find a compromise between these two objectives. The spatial domain watermarking techniques directly embed the watermark into the host image by altering the pixel values [8–11]. These methods generally are less robust to image and signal processing attacks and require low computational efforts, while frequency domain methods transform the representation of spatial domain into the frequency domain and then modify its frequency coefficients to embed the watermark. There are many transform domain watermarking techniques such as discrete cosine transforms (DCT) [12], discrete Fourier transforms (DFT) [13–14], discrete wavelet transforms (DWT) [15–17], and singular value decomposition (SVD) [2, 18–20]. These methods typically provide higher image imperceptibility and are much more robust to image manipulations, but the computational cost is higher than spatial domain watermarking methods. The performance of watermarking methods was further improved by combining two or more transformations [21–33]. The singular value decomposition (SVD) is extensively used in image watermarking field in recent years due to its features. However, various researchers pointed out the false positive detection problem in most of the SVD-based algorithms [7, 34–35]. To counter this problem, numerous researchers have proposed improved versions of SVD-based image watermarking schemes. A robust image watermarking scheme based on SVD that embeds the entire watermark is given in [20]. There are two versions of this scheme depending on the implementation of SVD, to entire cover image and block-wise. The imperceptibility of an image watermarking scheme using block based SVD proposed in [19] is improved by incorporating compensation operation. According to this scheme, the damage in the quality due to insertion of the watermark in the left singular vector matrix is compensated by modifying the right singular vector matrix. The host image is segmented into non-overlapping blocks of size  $4 \times 4$ ; then the embedding blocks are selected at random. The watermark bits are embedded by modifying the coefficients in the first column of the left singular vector matrix of the target blocks. The different regions within an image have different local features, so some visual models such as human visual system (HVS) may be incorporated in finding the suitable embedding regions to improve robustness while maintaining imperceptibility. Based on this concept, a blind SVD-based watermarking scheme is presented in [36]. The host image is segmented into non-overlapping blocks of size  $8 \times 8$ ; then the embedding blocks are selected based on the sum of visual and edge entropies. The watermark bits are embedded by modifying the coefficients in the first column of the left singular vector matrix of the target blocks. The above mentioned SVD-based watermarking schemes embed the entire watermark within the cover image. It has improved the reliability of the watermarking but sacrificed the transparency. Also, these schemes are applicable only for the black and white watermark. A watermarking scheme proposed in [32] is based on the fact that SVD subspace (left and right singular vectors) can preserve a significant amount of information about an image. Therefore, it embeds the principal component, multiplication of left singular vector matrix and the singular value matrix, of watermark into the host image instead of singular values of the watermark. On the same concept, Run et al. [33] introduced an image watermarking scheme embedding the principal component of the watermark in frequency domain (DCT and DWT domains, resp.). Also, an optimization technique is applied to get the optimal scaling factors for embedding. Though the features extracted are robust for so many attacks, the efficiency of watermarking approach also depends on the watermarking constant. There are so many approaches proposed in earlier towards the optimization of watermarking constant. PSO is an intelligent algorithm that using the stochastic, population-based computer algorithm for problem solving. Zheng [37] applied the PSO to search the embedding location of the integer DCT coefficients in a block to optimize the requirement of imperceptibility and robustness in watermarking. Vahedi [38] utilized the PSO method to search for the optimal energy of embedding watermark to balance the quality and robustness of watermarked image. In [39], a watermarking approach was proposed based on Genetic Algorithm (GA). In [23], GA was used for the selection of watermarking constant. Recently, particle swarm optimization (PSO) was evolved into the watermarking system. Hai Tao [40] applied PSO for the optimization of scaling factors to improve the robustness of watermarking scheme. 3-level DWT is used for

feature extraction and PSO for optimization. Though the PSO was used, there is a non-recoverable information loss due to the 3-level DWT. In [41], a novel watermarking approach was proposed by considering the PSO as an optimizer and Integer wavelet transform as a transform technique. Though the information loss was reduced in [41], there observed a reduced robustness in particular attacks like rotation, histogram equalization and cropping.

### III. PRELIMINARIES

#### A. Integer Wavelet Transform (IWT)

The main problem with wavelet transform is its inability to reduce the loss of information in the original image. For example, if any one of the block of original image having integer pixel values and transformed through a floating point wavelet transform. If the transformed coefficients are changed during the embedding, then this wavelet transform will not provide any guarantee about the integer values of that particular block. The truncation of floating point values will result in loss of information, i.e., the original image cannot be reconstructed effectively. Furthermore, the conventional wavelet transform is, in practice, implemented as a floating-point transform followed by a truncation or rounding since it is impossible to represent transform coefficients in their full accuracy. To avoid this problem, an invertible integer-to-integer wavelet transform based on lifting [41] is used in the proposed scheme. It maps integers to integers and does not cause any loss of information through forward and inverse transforms. The main advantage with Lifting based wavelet transforms is fast and accuracy. They are easy to implement and also doesnot require any additional memory.

The forward transform of a typical lifting scheme usually consists of three steps: split, prediction and update. Consider a signal:  $X = \{x(n), n \in \mathbb{Z}\}$  with  $x(n) \in \mathbb{R}$ . The implementation of the forward transform is illustrated as below:

(1) *Split*: The original signal  $X$  is split into two subsets: even indexed samples  $x_e$  and odd indexed sample  $x_o$  by means of a sample operation:

$$\begin{cases} x_e = x(2n) \\ x_o = x(2n + 1) \end{cases} \quad (1)$$

After the split operation is completed, the odd set and even set are obtained and the two sets are closely correlated. That is, adjacent samples are much more correlated than those far from each other. It is natural that one can build a good predictor for one set with other set.

(2) *Prediction*: Given the odd indexed samples  $x_o$ , a predictor  $P$  for the even indexed samples  $x_e$  can be designed:

$$\tilde{x}_o = P(x_e) \quad (2)$$

The difference denoted as  $d$  between the predicted results and the odd samples is considered as the detail coefficients of the signal  $x(n)$ , and it is expressed as:

$$d = x_o - \tilde{x}_o = x_o - P(x_e) \quad (3)$$

(3) *Update*: Knowing the even sample  $x_e$  and the detail coefficients  $d$ , the approximation coefficients  $c$  are recalculated using the updating operator  $U$  as:

$$c = x_e + U(d) \quad (4)$$

The inverse transform can immediately be derived from the forward transform by running the lifting scheme backwards. The block diagram of the lifting scheme is given in Figure 1.

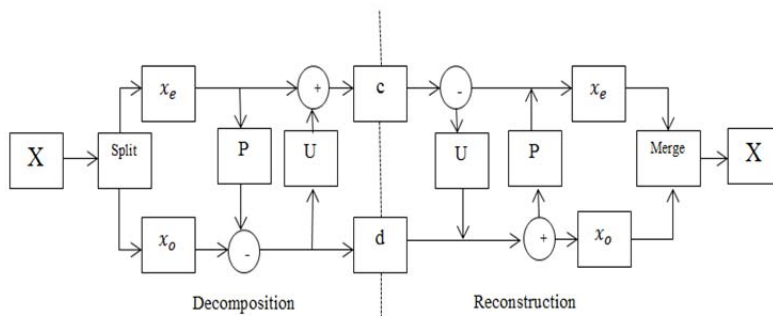


Figure.1 Lifting based decomposition and reconstruction

#### B. Singular Value Decomposition (SVD)

The singular valuedecomposition (SVD) [20] is a numerical analysis techniquebased on a theorem of linear algebra that decomposesa rectangular matrix into the product of three matrices:an orthogonal matrix ( $U$ ), a diagonal matrix ( $S$ ), and the transpose of an orthogonal matrix ( $V$ ). It may be consideredas a method of

transforming correlated data set into uncorrelated one that better explains the various relationships among the original data. Due to the unique features and attractive properties such as stability with little disturbance, SVD has been used in many signal and image processing applications such as image watermarking, image hiding, image compression, and noise reduction. The digital image is also a kind of signal which can be viewed as a matrix. According to the theory, the SVD of a rectangular matrix  $A$  of order  $m \times n$  is represented mathematically as

$$A = USV^T, \tag{5}$$

where  $UU^T = I_m$  and  $VV^T = I_n$ ; the columns of  $U$  are orthonormal eigenvectors of  $AA^T$ , the columns of  $V$  are orthonormal vectors of  $A^T A$ , and  $S$  is a diagonal matrix containing the square roots of the eigenvalues from  $U$  or  $V$  in descending order. If  $r$  ( $r \leq n$ ) is the rank of the matrix  $A$  then the elements of the diagonal matrix  $S$  satisfy the relation (6) and the matrix  $A$  can be written as (7):

$$\lambda_1 \geq \lambda_2 \geq \dots \geq \lambda_r > \lambda_{r+1} = \lambda_{r+2} = \dots = \lambda_n = 0, \tag{6}$$

$$A = \sum_{k=1}^r \lambda_k u_k v_k^T \tag{7}$$

Where  $u_k$  and  $v_k$  are the  $k_{th}$  eigenvector of  $U$  and  $V$  and  $\lambda_k$  is the  $k_{th}$  singular value.

### C. Genetic Algorithm

Genetic algorithm [39] is one of the most widely used artificial intelligent techniques belonging to the area of evolutionary computation. Usually, a simple GA is mainly composed of three operations: selection, genetic operation, and replacement. Initially, a population is randomly generated. The fitness function then uses objective values from objective function to evaluate the fitness of each chromosome. The fitter chromosome has the greater chance to survive during the evolution process. The objective function is problem specific; its objective value can represent the system performance index (e.g., an error). Next, a particular group of chromosomes is chosen from the population to be parents.

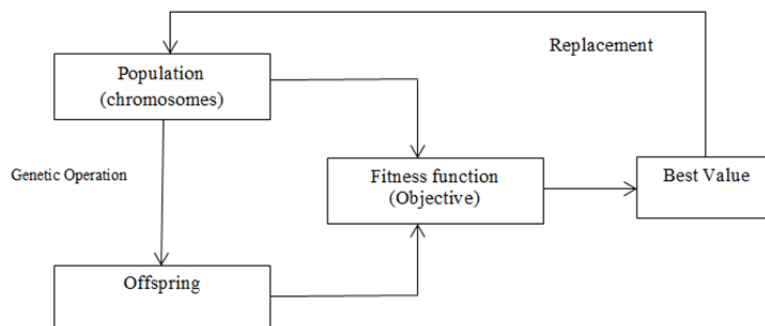


Fig.2. GA cycle

The offspring is then generated from these parents by using genetic operations, which normally are crossover and mutation. Similar to their parents, the fitness of the offspring is evaluated and used in replacement processes in order to replace the chromosomes in the current population by the selected offspring. The GA cycle is then repeated until a desired termination criterion is satisfied, for example, the maximum number of generations is reached or the objective value is below the threshold.

### D. Particle Swarm Optimization (PSO)

PSO [40] is motivated from the social behavior of organism such as bird flocking or fish schooling. It attempts to mimic the natural process of group communication in a wide range of domains and can be used to solve many different problems. Like other evolutionary algorithms, PSO is also a population-based search algorithm and initializes with a population of randomly generated solutions called particles which fly through the search space by updating the generation. Each particle represents a candidate solution to the optimization problem, and has a velocity and a position. The position of a particle is affected by both the best position visited by it and the position of the best particle in its neighbourhood. The best particle in the population is denoted by global best (gbest), while the best position that has been visited by the current particle is denoted by local best (pbest). Each particle is updated using the following equations:

$$v_i(n+1) = w_i v_i + c_1 rand_1(pbest - x_i(n)) + c_2 rand_2(gbest - x_i(n)) \tag{8}$$

$$x_i(n+1) = x_i(n) + v_i(n+1) \tag{9}$$

Where:

$x_i(n+1)$  and  $x_i(n)$  represent the current and the previous positions of particle  $i$

$v_i(n+1)$  and  $v_i(n)$  are the current and the previous velocity of the particle  $i$ .

$rand_1$  and  $rand_2$  are random numbers uniformly distributed within  $[0,1]$ .

$W$  is an inertia weight which controls the momentum of the particle.

In typical implementations of PSO algorithm, the value of  $w$  is decreased linearly from 1.0 to near 0 in each iteration. Commonly the inertia weight is set according to the following equation:

$$w_i = w_{max} - \frac{w_{max}-w_{min}}{iter_{max}} \cdot iter \quad (10)$$

Where:  $iter_{max}$  is the maximum number of iterations, and  $iter$  is the current number of iterations. Each particle in PSO shares the information with its neighbors. The updating equations (4) and (5) combine both of the cognition component of each particle and the social component of all the particles in a group. Although the speed of convergence is very fast, many experiments have shown that once PSO traps into local optimum, it is difficult for PSO to jump out of the local optimum.

#### IV. PROPOSED WATERMARKING SCHEME

This section illustrates the complete details about the mathematical formulation of the proposed watermarking scheme and its components. The system developed for proposed watermarking approach is shown in figure.3.

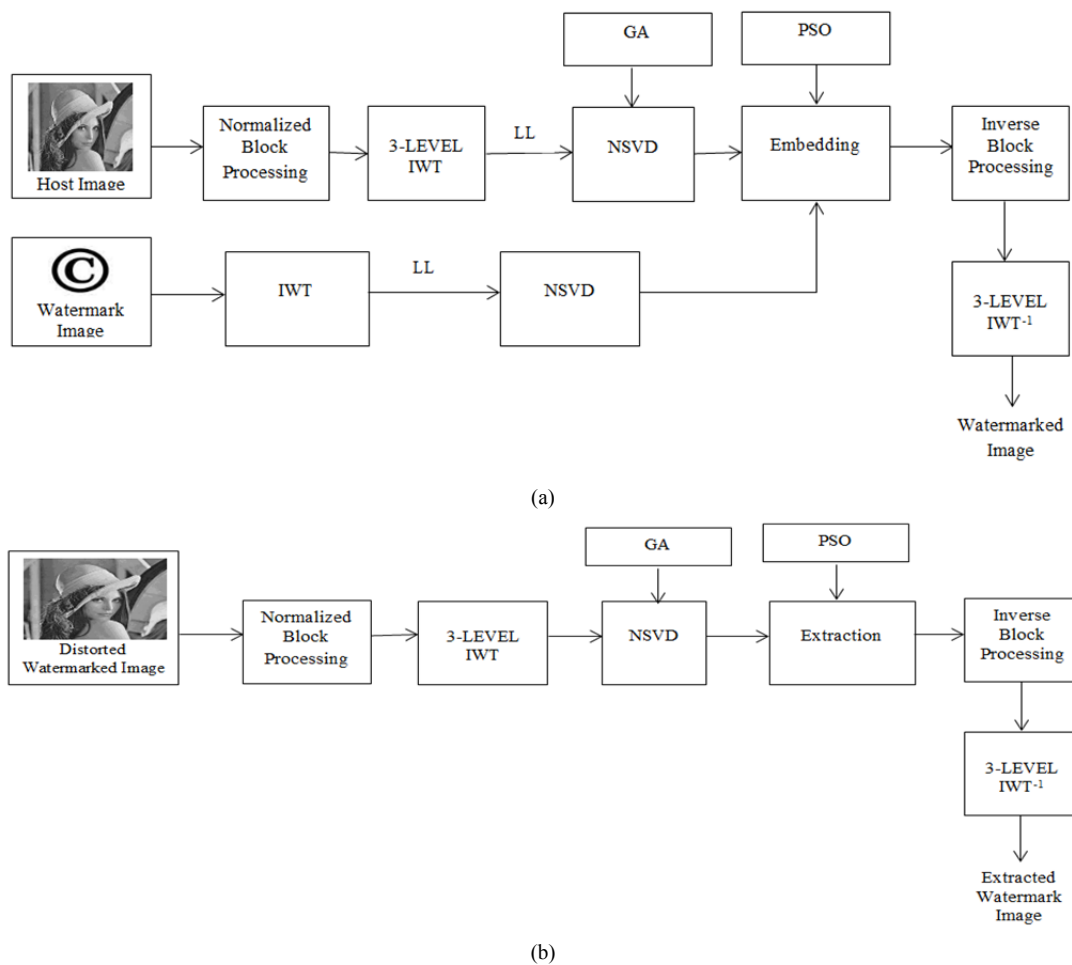


Figure.3. Proposed system for image watermarking (a) embedding phase (b) Extraction phase

##### A. Normalized Block Processing

The purpose of normalized block processing is to extract the invariant blocks of host image under rotation and flipping operations. The location of pixel values in a block may vary, but the elements of the blocks remain the same. To achieve it, pixels' locations of the image are redistributed and then some normalization procedures are performed. The block diagram of normalized block processing is shown in figure.4. Mathematically, it is formulated as follows.

Let  $I$  be the host image of size  $M \times N$  and  $W$  be the watermark image of size  $K \times L$ .

Step 1: Divide the host image  $I$  into four equal size blocks as  $B_1, B_2, B_3$  and  $B_4$ . Evaluate mean for every block such that  $m_{B_1}, m_{B_2}, m_{B_3}$  and  $m_{B_4}$  are the means of  $B_1, B_2, B_3$  and  $B_4$  respectively.

Step 2: Define a normalization mean matrix and sign matrix by summing and subtracting the means of all blocks, such as

$$N_i^m = \begin{bmatrix} N_1^m & N_2^m \\ N_3^m & N_4^m \end{bmatrix} = \begin{bmatrix} m_{B1} + m_{B2} + m_{B3} + m_{B4} & m_{B1} + m_{B2} - m_{B3} - m_{B4} \\ m_{B1} - m_{B2} + m_{B3} - m_{B4} & m_{B1} - m_{B2} - m_{B3} + m_{B4} \end{bmatrix} \quad (11)$$

$$N_i^s = \begin{bmatrix} N_1^s & N_2^s \\ N_3^s & N_4^s \end{bmatrix}, S = \text{sign} = \{-1, +1\} \quad (12)$$

Step 3: Obtain the normalized image by rearranging the original image according to the following rule,

$$\begin{cases} N_i(2k-1, 2l-1) = I(k, l) & 1 \leq k \leq M/2, 1 \leq l \leq N/2 \\ N_i(2k-1, 2l-N) = I(k, 3N/2-l+1) & 1 \leq k \leq M/2, N/2 \leq l \leq N \\ N_i(2k-M, 2l-1) = I(3M/2-k+1, l) & M/2 \leq k \leq M, 1 \leq l \leq N/2 \\ N_i(2k-M, 2l-N) = I(3M/2-k+1, 3N/2-l+1) & M/2 \leq k \leq M, N/2 \leq l \leq N \end{cases} \quad (13)$$

Step 4: Then perform the 3-level IWT on the obtained Normalized image and multiply the sub band of normalized image with normalized sign matrix as shown in Equation.(12) and denote the obtained matrix as

$$S = \begin{pmatrix} S_1 & S_2 \\ S_3 & S_4 \end{pmatrix}.$$

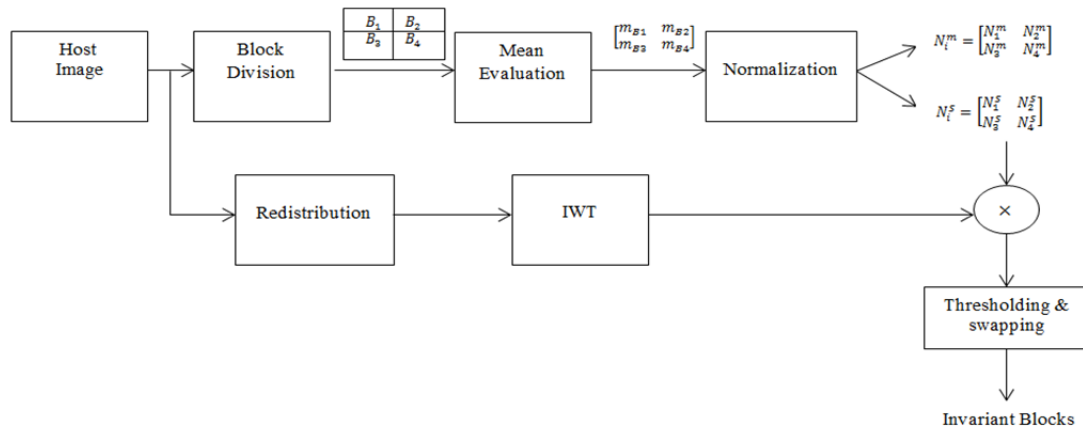


Fig.4. Normalized Block Processing & IWT

Step 5: The obtained matrix S will be invariant if the condition  $|N_3^m| < |N_2^m|$  is satisfied, otherwise, the swapping will be done and the final matrix was obtained by transposing the entire S matrix, i.e.,  $S = \begin{pmatrix} S_1^T & S_2^T \\ S_3^T & S_4^T \end{pmatrix}$ .

The final matrix S is the invariant wavelet domain; it is invariant to rotation and image flipping. That is, once the original is flipped or rotated the same wavelet domain can be achieved by above normalized block processing.

### B. Normalized SVD (NSVD)

From the SVD point of view it was noticed that every image matrix has the well-known SVD for any given single matrix A, the larger Singular Values (SVs) are very sensitive to variations in the image such as noise changes in the host image. Upon the occurrence of attack on the watermarked image, there may be effect on the pixel intensities. But the SVD are very sensitive to these variations. To alleviate the variations in image, a normalized SVD approach is proposed with mainly two ideas such as the weights of host image  $uv^T$  should be deflated since they are every sensitive to the variations in the image itself and weights of base images  $uv^T$  corresponding to relatively small  $\lambda_i$ 's should be inflated, since they may be less sensitive to the variations within the image.

This can be illustrated through the following concept. Let's consider the image I is denoted as  $I = [i_1, i_2, \dots, i_r]^T$ , where  $i_i^T$  is a  $1 \times c$  row vector that represents the  $i$ th row of matrix I, then

$$V^T C_{row} V = S^2 \quad (14)$$

Where

$$C_{row} = I^T I = \sum_{i=1}^r i_i i_i^T \quad (15)$$

I.e.,  $v_j$  is the eigenvector of the covariance matrix  $C_{row}$  corresponding to Eigen value  $\lambda_j^2, j = 1, 2, \dots, k$ . Similarly, Let's consider the image  $I$  is denoted as  $I = [i_1, i_2, \dots, i_c]^T$ , where  $i_i^T$  is a  $r \times 1$  row vector that represents the  $i$ th Colom of matrix  $I$ , then

$$U^T C_{row} U = S^2 \quad (16)$$

Where

$$C_{row} = I^T I = \sum_{i=1}^r i_i i_i^T \quad (17)$$

I.e.,  $u_j$  is the eigenvector of the covariance matrix  $C_{row}$  corresponding to Eigen value  $\lambda_j^2, j = 1, 2, \dots, k$ .

Hence, the  $\lambda_i$ 's should be inflated, since they may be less sensitive to the variations within the image, a new SVD formulation can be derived by modifying the standard SVD evaluation (shown in equation.(5)) as,

$$A = US^\gamma V^T \quad (18)$$

Where  $U, S$  and  $V$  are the corresponding matrices in Eq. (1), and  $\gamma$  is the normalizing constant. In order to achieve the requirements, the  $\gamma$  needs to satisfy the following condition.

$$0 \leq \gamma \leq 1 \quad (19)$$

### C. Embedding Process

Step 1: Let  $W$  be the watermark image. Perform one level IWT on the Watermark image  $W$

$$W \rightarrow \{W_{LL}, W_{LH}, W_{HL}, W_{HH}\}$$

Step 2: perform block processing on the LL band  $W_{LL}$ . Evaluate an optimal normalization constant ( $\gamma$ ) through the GA algorithm and then perform the normalized SVD (NSVD) on the obtained LL band of Watermark image  $W$

$$W_{LL}(i, j) \rightarrow U_w(i, j) S_w^\gamma(i, j) V_w^T(i, j)$$

Step 3: Obtain principal component by multiplying the components  $U_w$  and  $S_w^\gamma$ .

$$W_{US}(i, j) = U_w S_w^\gamma$$

Let  $W_{US}(i, j)$  be the principal component at pixel position  $(i, j)$ , where  $i, j = 1, 2, \dots, N$ .

Step 4: Apply normalized block processing on the original host image to obtain normalized image.

Step 5: Apply three level IWT on the normalized image.

$$N_I \rightarrow \{N_{ILL}, N_{ILH}, N_{IHL}, N_{IHH}\}$$

Step 6: Evaluate an optimal normalization constant ( $\gamma$ ) through the GA algorithm and then perform the normalized SVD (NSVD) on the obtained LL band of Normalized Host image having invariant blocks to get the largest singular value  $\lambda_{max}$ . Let  $ll(i, j)$  be the invariant block at position  $(i, j)$ .

$$ll(i, j) \rightarrow U_{ll} S_{ll}^\gamma V_{ll}^T$$

Where  $S = \text{diag}(\lambda_k), k = 1, 2, \dots, N$ . The watermark principal component is embedded into the host image by modifying the largest singular value.

Step 7: Embed the watermark principal component into the largest singular value of host image for each image block  $(i, j)$  using the following formula:

$$\lambda_{max}^m = \lambda_{max}(i, j) + \alpha W_{US}(i, j)$$

Where  $\lambda_{max}^m$  is the modified singular value of image block  $(i, j)$  and  $\alpha$  is the watermarking constant can be obtained through the PSO.

Step 8: perform inverse SVD on the obtained singular values of every block  $(i, j)$ .

$$ll^m(i, j) \leftarrow U_{ll} (S_{ll}^\gamma)^m V_{ll}^T$$

Where  $(S_{ll}^\gamma)^m$  is the modified singular matrix for the block at position  $(i, j)$ .

Step 9: reconstruct the complete LL band after getting individual blocks. Thus the reconstructed LL band will be a modified band of the normalized image, can be represented as  $N_{ILL}^m$ .

Step 10: perform Inverse IWT (IIWT) to reconstruct the normalized watermarked image ( $N_I^W$ ).

$$N_I^W \leftarrow \{N_{ILL}^m, N_{ILH}, N_{IHL}, N_{IHH}\}$$

Step 11: perform inverse redistribution and normalization to obtain the final watermarked image  $I_W$ .

### D. Extraction Process

The extraction process is applied on the distorted watermarked image,  $I_W^*$ , to extract the watermark image and after the extraction the obtained watermark image is also distorted and can be represented as  $W^*$ . The following procedural steps were followed for extraction purpose.

Step 1: Apply the normalized block processing on the distorted watermarked image ( $I_W^*$ ) to obtain the distorted normalized watermarked image ( $N_{I_W}^*$ ).

Step 2: Apply three level IWT on the distorted & normalized watermarked image ( $N_{I_W}^*$ ).

$$N_{I_W}^* \rightarrow \{N_{I_W}^{*LL}, N_{I_W}^{*LH}, N_{I_W}^{*HL}, N_{I_W}^{*HH}\}$$

Step 3: Divide the approximate band into equal size non-overlapping blocks which can be denoted as  $ll^*(i, j), i, j = 1, 2, \dots, N$ .

Step 4: Apply NSVD on every block  $ll^*(i, j)$  to obtain the maximum singular value  $\lambda_{max}^*(i, j)$ .

$$ll^*(i, j) \rightarrow U_{ll}^* (S_{ll}^*)^{\gamma} (V_{ll}^*)^T$$

Step 5: extract the distorted principal component  $W_{US}^*(i, j)$  through the following formula as,

$$W_{US}^*(i, j) = \frac{(\lambda_{max}^*(i, j) - \lambda_{max}(i, j))}{\alpha}$$

Step 6: Perform inverse NSVD by multiplying the obtained principal component  $W_{US}^*(i, j)$  with  $V_W^T$  to obtain a distorted block  $W_{ll(i,j)}^*$

$$W_{ll(i,j)}^* \leftarrow W_{US}^*(i, j) V_W^T$$

Step 7: Reconstruct the distorted LL band of watermark image by merging the all obtained distorted blocks.

$$W_{LL}^* \leftarrow \{W_{ll(i,j)}^*\}$$

Step 8: Perform Inverse IWT to obtain the final extracted watermark image  $W^*$ .

$$W^* \leftarrow \{W_{LL}^*, W_{LH}, W_{HL}, W_{HH}\}$$

Where  $W^*$  is the extracted watermark.

This entire process repeats for entire population generated for optimization in GA and PSO.

### V.SIMULATION RESULTS

In this section, the performance of proposed approach was analyzed under various experiments. For performance evaluation, three host images and two watermark images are considered and shown in figure.5 and figure.6 respectively. To investigate the robustness of proposed approach, the watermarked image was subjected to eight attacks such as: (1) Gaussian noise Attack (GNA) with noise variance as 0.001, 0.01 and 0.1, (2) salt & pepper noise attack (SPA) with noise variance as 0.001, 0.01 and 0.1, (3) Median Filtering attack (MFA) with average window size of 3X3 and 7X7, (4) Histogram Equalization attack (HEA), (5) Rotation attack (RA) with rotation of  $30^0$  and  $45^0$ , (6) Contrast Enhancement attack (CEA) with contrast limit of 0.03 and 0.05, (7) cropping attack (CA) and (8) Scalling Attack (SA) with Nearest Neighbor, bi-linear and bi-cubic.

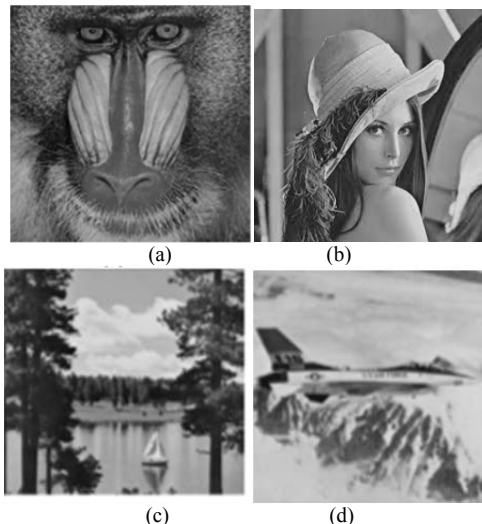


Fig.5 Host images (a) Baboon, (b) Lena (c) Lake (d) Plane

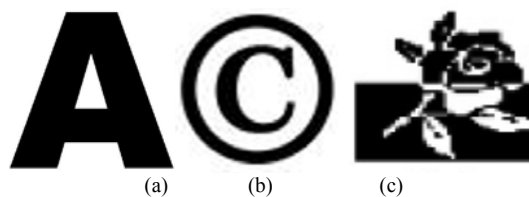


Fig.6 Watermark images (a) Character (b) Logo (c) Rose



To evaluate the performance of proposed approach, four performance metrics such as Mean Square Error (MSE), Peak Signal to Noise Ratio (PSNR), Normalized Correlation (NC) and Structural Similarity Index Measure (SSIM) were considered and the respective mathematical formulation is given as,

$$MSE = \frac{1}{M \times N} \sum_{i=1}^M \sum_{j=1}^N (w(i,j) - w^*(i,j))^2 \quad (20)$$

Where

$w$  = original watermark image

$w^*$  = extracted watermark image

$$PSNR = 10 * \log(255^2 / MSE) \quad (21)$$

$$NC = \frac{\sum_{i=1}^M \sum_{j=1}^N w(i,j) * w^*(i,j)}{\sqrt{(\sum_{i=1}^M \sum_{j=1}^N w(i,j)^2) * (\sum_{i=1}^M \sum_{j=1}^N w^*(i,j)^2)}} \quad (22)$$

$$SSIM = \frac{\sum_i \sum_j w(i,j) \otimes w^*(i,j)}{\sqrt{\sum_i \sum_j (w(i,j))^2}} \quad (23)$$

The NC is also used for the evaluation of fitness function of PSO. The fitness function of PSO is defined as

$$fitness(s_j) = 1 - Average(NC_j)$$

$$NC_j = \frac{1}{n_{attack}} \sum_{k=1}^{n_{attack}} NC(w, w_j^{*,k}) \quad (24)$$

Where  $w_j^{*,k}$  represents the extracted watermark through the proposed approach characterized by the position of the  $j_{th}$  particle. The smaller fitness value means the better robustness. Let,  $n_{attack}$  signifies the number of attacks, here the  $n_{attack}$  is set to 8. Because, totally eight types of attacks are simulated in the simulation.

Performance metrics was evaluated for both No attack and Attack scenarios. At both phases, the proposed approach was compared with T. Naheed et.al [6] and S.P.Rao et.al[41].

**A. No attack scenario**

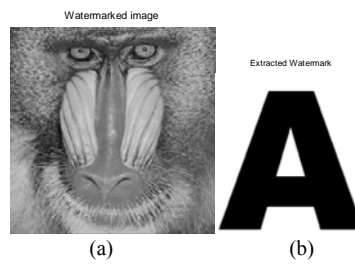


Fig.7. (a) watermarked image (b) extracted watermark image

**B. Attack Scenario**

**1. Gaussian Noise Attack (variance=0.001, 0.01, 0.1)**

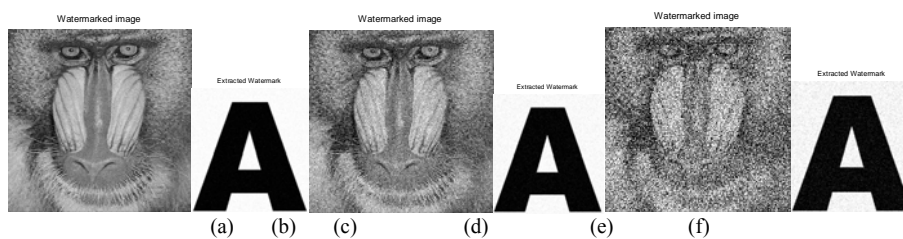


Fig.8. Obtained results in the case of gaussian noise attack scenario

**2. Salt & Pepper Noise Attack (variance=0.001, 0.01, 0.1)**

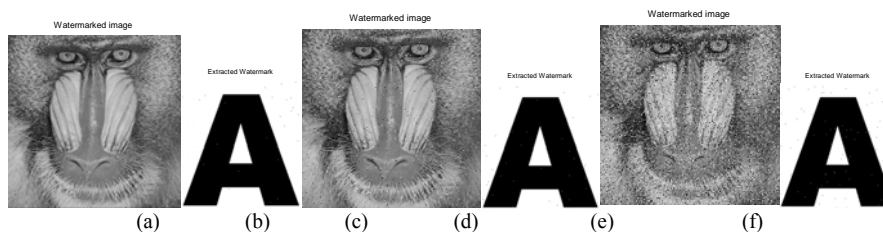


Fig.9. Obtained results in the case of salt & pepper noise attack scenario

### 3. Median Filtering Attack of average size 3X3 and 7X7

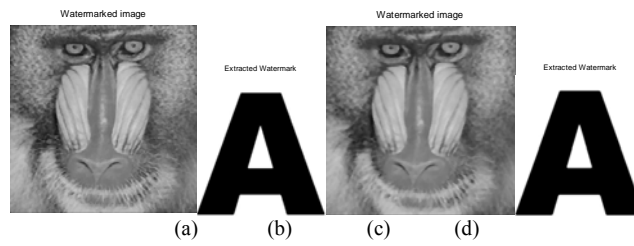


Fig.10. Obtained results in the case of Median Filtering attack scenario

### 4. Histogram Equalization Attack

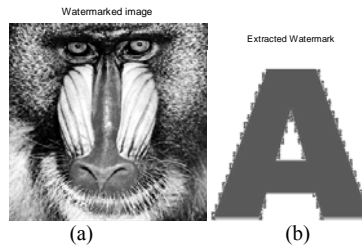


Fig.11. Obtained results in the case of Histogram Equalization attack scenario

### 5. Rotation Attack at 30° and 45°

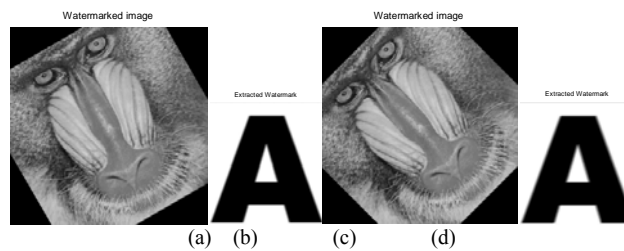


Fig.12. Obtained results in the case of Rotation attack scenario

### 6. Contrast Enhancement Attack at contrast limit = 0.03 and 0.05

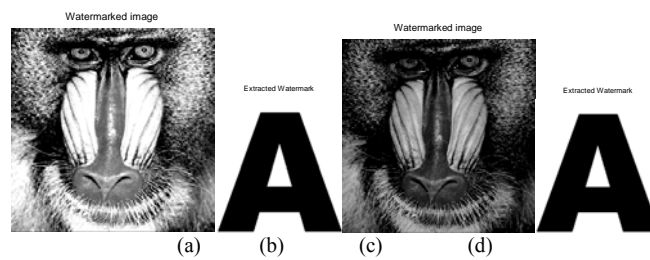


Fig.13. Obtained results in the case of Contrast Enhancement attack scenario

### 7. Cropping Attack

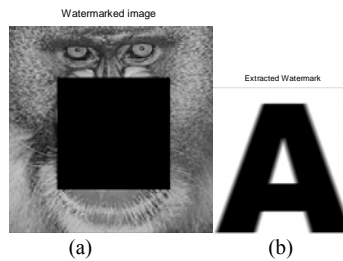


Fig.14. Obtained results in the case of Cropping attack scenario

8. Scalling Attack at nearest neighbor, bi-linear and bi-cubic

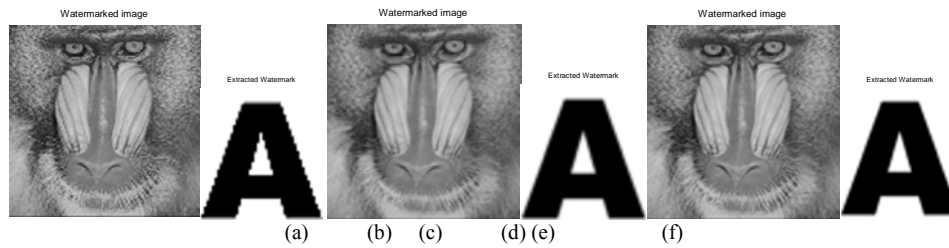


Fig.15. Obtained results in the case of scalling attack scenario

The evaluated PSNR, MSE, NC and SSIM of all the attack scenarios are represented in the following tables.

Table. 1. Performance analysis of proposed approach in the case of no attack scenario

Metrics	Baboon with character			Lena with Logo		
	S.P.Rao.et.al [41]	T.N.et.al [6]	Proposed	S.P.Rao.et.al [41]	T.N.et.al [6]	Proposed
PSNR	47.9936	48.5514	52.7485	48.8982	49.2232	53.0287
MSE	1.0321	0.9077	0.3453	0.8380	0.7776	0.3238
NC	0.9789	0.9825	0.9869	0.9812	0.9832	0.9876
SSIM	0.9824	0.9857	0.9892	0.9842	0.9858	0.9883

Table.2. Performance analysis of proposed approach for gaussian noise attack while varying noise variance

Variance	Metrics	Baboon with character			Lena with Logo		
		S.P.Rao.et.al [41]	T.N.et.al [6]	Proposed	S.P.Rao.et.al [41]	T.N.et.al [6]	Proposed
0.001	PSNR	47.7512	48.1418	50.9879	47.9985	48.6698	51.2275
	MSE	1.0913	0.9975	0.5180	1.0309	0.8833	0.4902
	NC	0.8998	0.9012	0.9119	0.9005	0.9196	0.9238
	SSIM	0.9644	0.9688	0.9785	0.9648	0.9698	0.9798
0.01	PSNR	47.2276	47.4478	50.2041	47.3325	48.3363	50.8689
	MSE	1.2312	1.1703	0.6204	1.2018	0.9538	0.5323
	NC	0.8845	0.8898	0.9069	0.8812	0.8856	0.9172
	SSIM	0.9628	0.9637	0.9735	0.9621	0.9645	0.9766
0.1	PSNR	46.9898	47.0549	49.9338	47.0201	48.1298	50.0371
	MSE	1.3005	1.2811	0.6602	1.2914	1.0002	0.6647
	NC	0.8797	0.8835	0.9013	0.8809	0.8824	0.9022
	SSIM	0.9583	0.9615	0.9638	0.9606	0.9632	0.9721

Table.3. Performance analysis of proposed approach for salt & pepper noise attack while varying noise variance

Variance	Metrics	Baboon with character			Lena with Logo		
		S.P.Rao.et.al [41]	T.N.et.al [6]	Proposed	S.P.Rao.et.al [41]	T.N.et.al [6]	Proposed
0.001	PSNR	46.7473	47.2536	49.8754	46.8891	47.7471	49.9963
	MSE	1.3752	1.2238	0.6692	1.3310	1.0924	0.6508
	NC	0.9618	0.9635	0.9685	0.9635	0.9655	0.9681
	SSIM	0.9456	0.9489	0.9519	0.9486	0.9498	0.9522
0.01	PSNR	46.2234	46.8481	49.0286	46.3814	47.1789	49.3399
	MSE	1.5515	1.3436	0.8132	1.4960	1.2451	0.7570
	NC	0.9601	0.9624	0.9646	0.9585	0.9623	0.9651
	SSIM	0.9417	0.9456	0.9490	0.9422	0.9466	0.9507
0.1	PSNR	45.8746	46.1325	48.2358	46.1238	46.8576	48.8339
	MSE	1.6812	1.5843	0.9761	1.5835	1.3407	0.8505
	NC	0.9519	0.9559	0.9573	0.9515	0.9565	0.9595
	SSIM	0.9367	0.9396	0.9420	0.9369	0.9402	0.9469

Table.4. Performance analysis of proposed approach for Median Filtering attack scenario with varying size

Variance	Metrics	Baboon with character			Lena with Logo		
		S.P.Rao.et.al [41]	T.N.et.al [6]	Proposed	S.P.Rao.et.al [41]	T.N.et.al [6]	Proposed
3X3	PSNR	47.1015	47.5589	48.5680	47.2021	47.8680	48.7990
	MSE	1.2674	1.1407	0.9042	1.2384	1.0624	0.8574
	NC	0.9555	0.9569	0.9589	0.9563	0.9577	0.9586
	SSIM	0.9383	0.9399	0.9478	0.9386	0.9419	0.9461
7X7	PSNR	46.5312	47.1013	48.1090	46.3158	47.1519	48.3960
	MSE	1.4453	1.2675	1.0050	1.5188	1.2528	0.9408
	NC	0.9499	0.9533	0.9542	0.9493	0.9528	0.9567
	SSIM	0.9255	0.9267	0.9301	0.9229	0.9296	0.9355

Table.5. Performance analysis of proposed approach for Histogram Equalization attack

Metrics	Baboon with character			Lena with Logo		
	S.P.Rao.et.al [41]	T.N.et.al [6]	Proposed	S.P.Rao.et.al [41]	T.N.et.al [6]	Proposed
PSNR	27.6349	29.3685	31.9785	27.2241	29.2247	31.8555
MSE	112.0961	75.2022	41.2316	123.2169	77.7329	42.4161
NC	0.8839	0.8869	0.8992	0.8823	0.8855	0.8986
SSIM	0.9317	0.9346	0.9379	0.9274	0.9327	0.9366

Table.6. Performance analysis of proposed approach for Rotation attack scenario with varying angle of rotation

Rotation	Metrics	Baboon with character			Lena with Logo		
		S.P.Rao.et.al [41]	T.N.et.al [6]	Proposed	S.P.Rao.et.al [41]	T.N.et.al [6]	Proposed
30°	PSNR	22.3963	24.5689	30.3252	21.5335	23.3312	30.1128
	MSE	374.49	227.68	60.3338	456.80	301.96	63.3578
	NC	0.8748	0.8965	0.9245	0.8797	0.8814	0.9287
	SSIM	0.8819	0.8956	0.9328	0.8831	0.8844	0.9338
45°	PSNR	22.2285	24.4578	30.1285	21.3388	23.1102	30.0360
	MSE	389.25	232.97	63.1292	477.74	317.73	64.4882
	NC	0.8652	0.8766	0.9222	0.8723	0.8786	0.9254
	SSIM	0.8796	0.8823	0.9313	0.8744	0.8794	0.9321

Table.7. Performance analysis of proposed approach in the case of Contrast Enhancemnet attack with varying contrast limit

Limit	Metrics	Baboon with character			Lena with Logo		
		S.P.Rao.et.al [41]	T.N.et.al [6]	Proposed	S.P.Rao.et.al [41]	T.N.et.al [6]	Proposed
0.03	PSNR	30.2145	31.7728	32.7463	29.6336	31.9696	32.8389
	MSE	61.8914	43.2315	34.5502	70.7490	41.3162	33.8213
	NC	0.9247	0.9278	0.9293	0.9298	0.9322	0.9356
	SSIM	0.9566	0.9599	0.9647	0.9589	0.9636	0.9670
0.05	PSNR	29.9985	30.2252	31.9697	28.9631	30.0028	31.9492
	MSE	65.0475	61.7391	41.3152	82.5601	64.9831	41.5107
	NC	0.9183	0.9196	0.9277	0.9189	0.9245	0.9281
	SSIM	0.9537	0.9587	0.9623	0.9522	0.9629	0.9658

Table.8. Performance analysis of proposed approach for cropping attack

Metrics	Baboon with character			Lena with Logo		
	S.P.Rao.et.al [41]	T.N.et.al [6]	Proposed	S.P.Rao.et.al [41]	T.N.et.al [6]	Proposed
PSNR	19.8634	21.6631	24.5789	18.8524	21.0129	24.1329
MSE	671.02	443.37	226.56	846.91	514.98	251.06
NC	0.7285	0.7358	0.7449	0.7238	0.7339	0.7396
SSIM	0.8125	0.8229	0.8494	0.8093	0.8156	0.8379

Table.9. Performance analysis of proposed approach for scalling attack scenario with various scalling techniques

Scaling technique	Metrics	Baboon with character			Lena with Logo		
		S.P.Rao.et.al [41]	T.N.et.al [6]	Proposed	S.P.Rao.et.al [41]	T.N.et.al [6]	Proposed
Nearest neighbor	PSNR	32.9721	33.2147	37.3339	32.3396	32.8985	37.2327
	MSE	32.7997	31.0178	12.0141	37.9420	33.3603	12.2973
	NC	0.9641	0.9668	0.9721	0.9655	0.9673	0.9682
	SSIM	0.9613	0.9638	0.9749	0.9647	0.9680	0.9687
Bi-linear	PSNR	34.6685	34.9967	38.4418	34.2285	35.2287	38.3387
	MSE	22.1937	20.5783	9.3089	24.5601	19.5079	9.5326
	NC	0.9688	0.9699	0.9133	0.9695	0.9719	0.9138
	SSIM	0.9633	0.9683	0.9758	0.9698	0.9732	0.9757
Bi-cubi	PSNR	36.2215	36.5878	39.6321	36.1328	36.3367	39.2124
	MSE	15.5214	14.2659	7.0955	15.8416	15.1151	7.7954
	NC	0.9731	0.9751	0.9766	0.9721	0.9736	0.9765
	SSIM	0.9745	0.9772	0.9784	0.9788	0.9790	0.9794

A case study was carried out by considering the charcater image as watermark and the Baboon image as host. The obtained PSNR, NC and SSIM are represented in the figure.16. Similarly, a one more case study is carried out for Logo and Lena as watermark and host images. The obatined results are shown in figure.17.

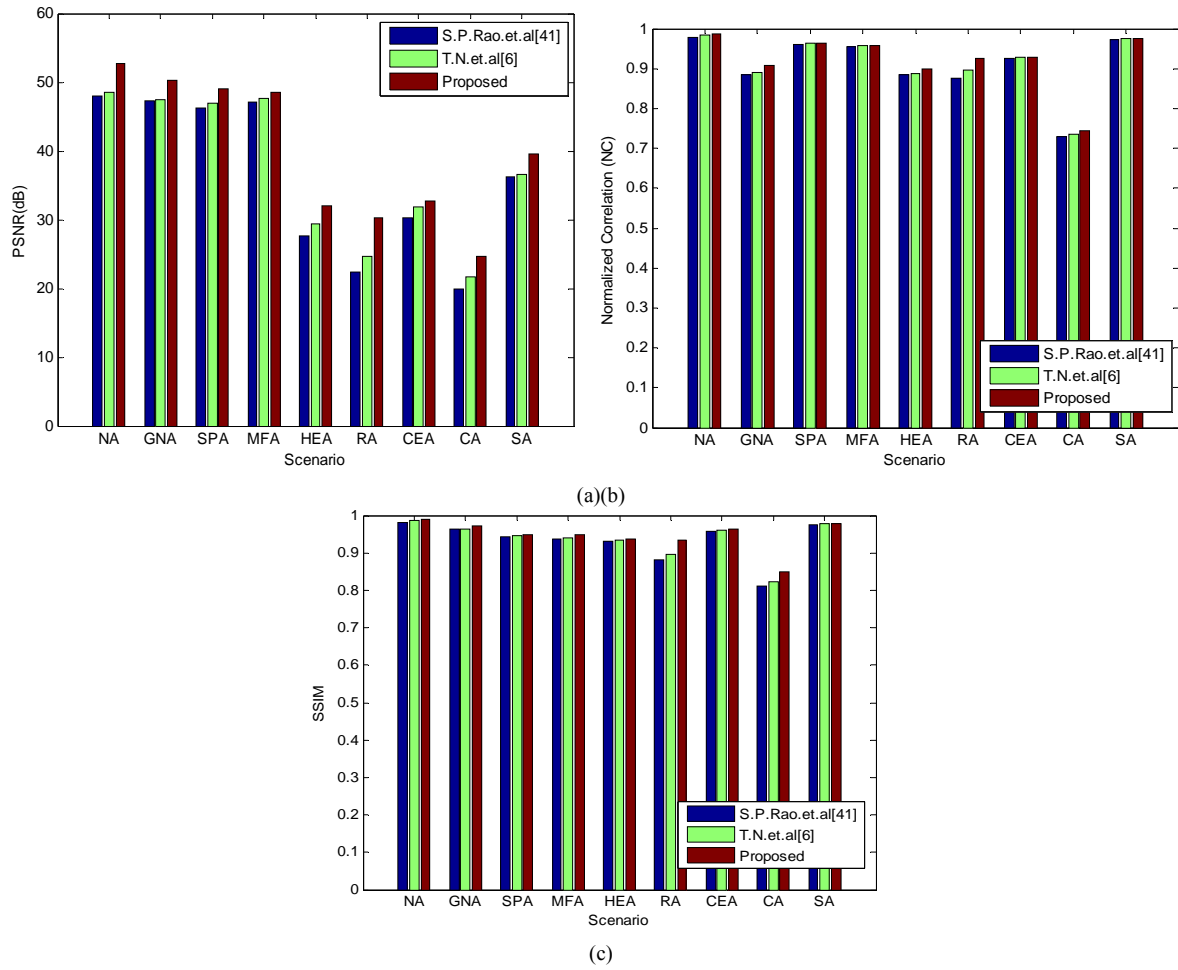
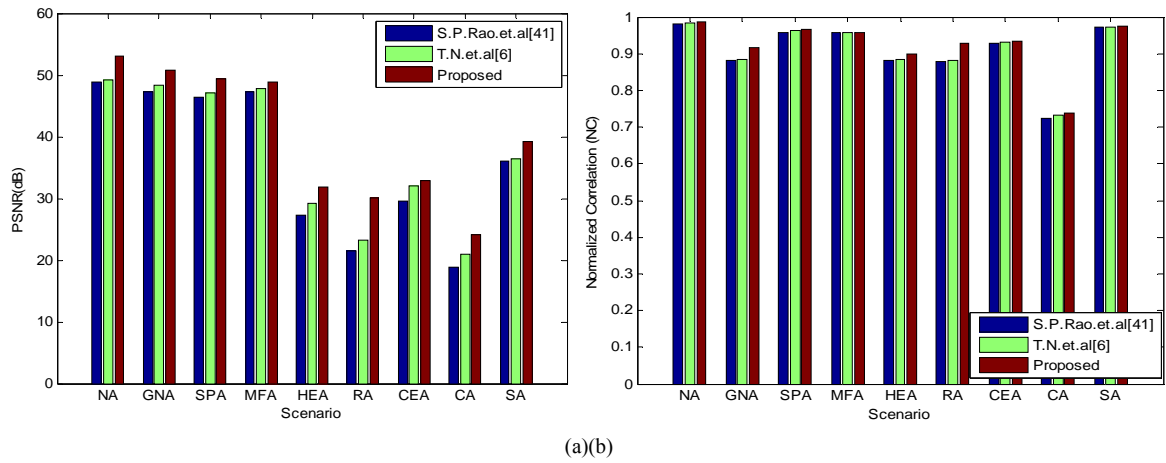
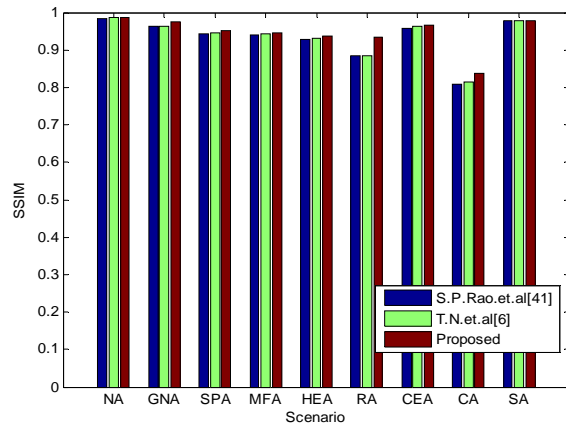


Fig.16. Performance metrics for the test case of Baboon image as a host and Character image as a watermark (a) PSNR, (b) NC and (c) SSIM

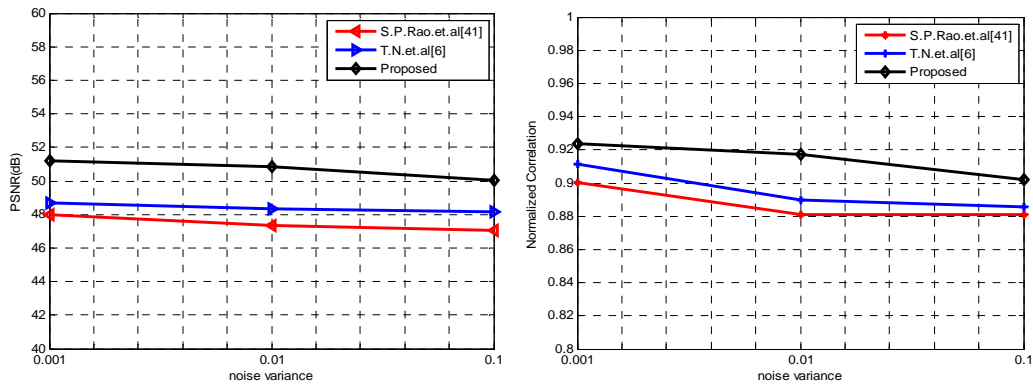




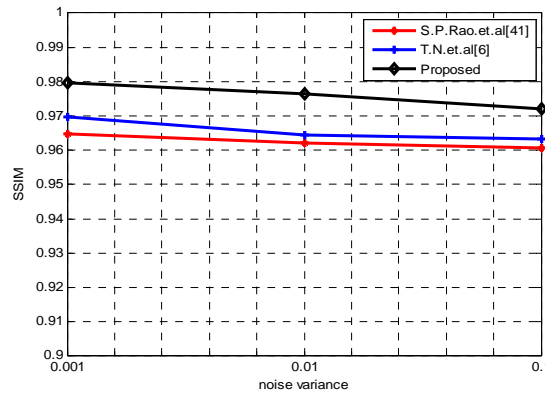
(c)

Fig.17. Performance metrics for the test case of Lena image as a host and Logo image as a watermark (a) PSNR, (b) NC and (c) SSIM

Another case study is performed over conventional and proposed approaches by varying the noise variance over gaussian noise attack and the obtained PSNR, NC and SSIM are represented in figures.18. In this case the Lena image is considered as host and the Rose image is considered as watermark.



(a)(b)



(c)

Fig.18. Performance metrics for the test case of Lena image as a host and Logo image as a watermark for varying gaussian noise variance (a) PSNR, (b) NC and (c) SSIM

From the fig.18(a), it can be observed that the PSNR is gradually decreasing with increasing noise variance. At every instant of noise variance, the proposed approach is observed to be efficient, because the proposed approach obtained an increased PSNR compared to conventional approaches. Similarly, fig.18 (b) and fig.18(c) elevate the robustness of the proposed approach with respect to NC and SSIM.

The performance of the watermarking scheme will vary with the noise variance under the salt & pepper noise attack also. The noise variance is varied as 0.001, 0.01 and 0.1 and the obtained PSNR, NC and SSIM considering the Lena as a host and Logo as a watermark is represented in the figure.19.

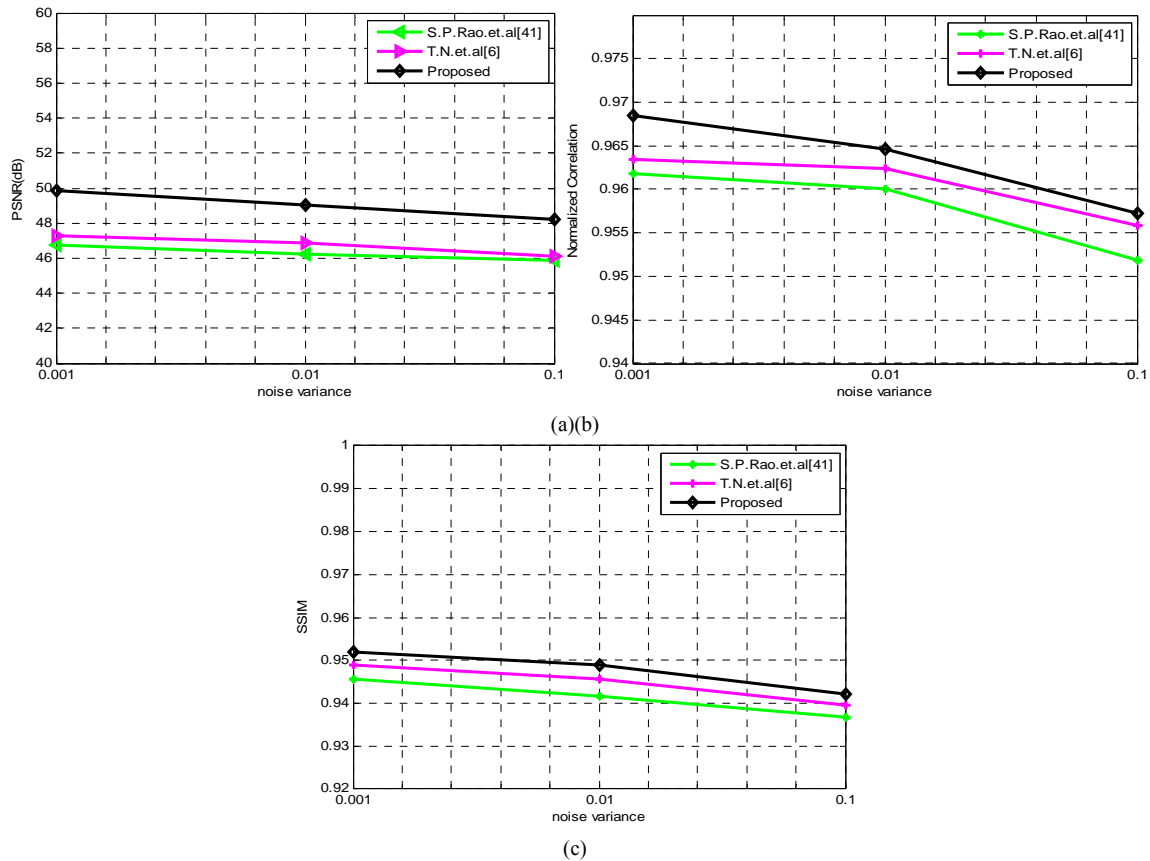


Fig.19. Performance metrics for the test case of Lena image as a host and Logo image as a watermark for varying salt & pepper noise variance (a) PSNR, (b) NC and (c) SSIM

From the above performance analysis, it can be observed that the proposed approach showing a superior performance over conventional approaches in all cases. It is observed that the proposed approach shown an excellent performance in the case of rotation attack. In that rotation attack scenario, the proposed approach achieved an improved PSNR of 4-5dB on an average.

## VI. CONCLUSION

In this paper, a new watermarking approach was proposed to enhance the robustness in various applications and also to ensure the imperceptibility. A combination of artificial intelligent techniques such as GA and PSO were utilized here to improve the performance. In this paper, the GA is accomplished at the feature extraction phase to find the optimum features which are roust for any type of attacks and PSO is used for enhancing the strength of watermark process. Along with these methods, at preprocessing stage, the original host image is subjected to a normalization process, particularly to obtain the features which are invariant. Then the further process is accomplished on the obtained invariant features. This normalization increases the robustness of watermarking approach in the case or rotation attack specifically. Finally, a performance evaluation is carried out by considering various host and watermark images and the performance metrics PSNR, MSE, NC and SSIM were evaluated to verify the proposed approach. A comparative analysis is also carried out by comparing the proposed approach with conventional approaches at various cases and proved as the proposed approach is robust. Thus, the proposed scheme has satisfied the robustness, and imperceptibility, requirements that are essential for a robust watermarking scheme.

## VII. REFERENCES

- [1] I. J. Cox, J. Kilian, F. T. Leighton, and T. Shamon, "Secure spread spectrum watermarking for multimedia," *IEEE Transactions on Image Processing*, vol. 6, no. 12, pp. 1673–1687, 1997.
- [2] R. Liu and T. Tan, "An SVD-based watermarking scheme for protecting rightful ownership," *IEEE Transactions on Multimedia*, vol. 4, no. 1, pp. 121–128, 2002.
- [3] M. L. Miller, I. J. Cox, J.-P. M. G. Linnartz, and T. Kalker, "A review of watermarking principles and practices," in *Digital Signal Processing in Multimedia Systems*, pp. 461–485, 1999.
- [4] E. Hussein and M. A. Belal, "Digital watermarking techniques, applications and attacks applied to digital media: a survey," *International Journal of Engineering Research and Technology*, vol. 1, no. 7, pp. 1–8, 2012.
- [5] A. Khan, A. Siddiqa, S.Munib, and S. A.Malik, "A recent survey of reversible watermarking techniques," *Information Sciences*, vol. 279, pp. 251–272, 2014.
- [6] Talat Naheed, "Intelligent reversible watermarking technique in medical images using GA and PSO", *Optik - Int. J. Light Electron*, 2014.

- [7] Asha Rani, "A Zero-Watermarking Scheme using Discrete Wavelet Transform", in Proc., of International Conference on Eco-friendly Computing and Communication Systems (ICECCS), 2015.
- [8] L.-D. Li and B.-L. Guo, "Localized image watermarking in spatial domain resistant to geometric attacks," *AEU: International Journal of Electronics and Communications*, vol. 63, no. 2, pp. 123–131, 2009.
- [9] Q. Su, Y. Niu, Q. Wang, and G. Sheng, "A blind color image watermarking based on DC component in the spatial domain," *Optik*, vol. 124, no. 23, pp. 6255–6260, 2013.
- [10] C.-H. Yang, C.-Y. Weng, S.-J. Wang, and H.-M. Sun, "Adaptive data hiding in edge areas of images with spatial LSB domain systems," *IEEE Transactions on Information Forensics and Security*, vol. 3, no. 3, pp. 488–497, 2008.
- [11] S. S. Jamal, T. Shah, and I. Hussain, "An efficient scheme for digital watermarking using chaotic map," *Nonlinear Dynamics*, vol. 73, no. 3, pp. 1469–1474, 2013.
- [12] S. D. Lin, S.-C. Shie, and J. Y. Guo, "Improving the robustness of DCT-based image watermarking against JPEG compression," *Computer Standards and Interfaces*, vol. 32, no. 1-2, pp. 54–60, 2010.
- [13] B. Chen, G. Coatrieux, G. Chen, X. Sun, J. L. Coatrieux, and H. Shu, "Full 4-D quaternion discrete Fourier transform based watermarking for color images," *Digital Signal Processing*, vol. 28, no. 1, pp. 106–119, 2014.
- [14] J. Lang and Z.-G. Zhang, "Blind digital watermarking method in the fractional Fourier transform domain," *Optics and Lasers in Engineering*, vol. 53, pp. 112–121, 2014.
- [15] E. H. Elshazly, O. S. Faragallah, A. M. Abbas, "Robust and secure fractional wavelet image watermarking," *Signal, Image and Video Processing*, Vol.9, pp.89–98, December 2015.
- [16] L. Li, H.-H. Xu, C.-C. Chang, and Y.-Y. Ma, "A novel image watermarking in redistributed invariant wavelet domain," *Journal of Systems and Software*, vol. 84, no. 6, pp. 923–929, 2011.
- [17] N. Liu, H. Li, H. Dai, D. Guo, and D. Chen, "Robust blind image watermarking based on chaotic mixtures," *Nonlinear Dynamics*, vol. 80, no. 3, pp. 1329–1355, 2015.
- [18] M.-Q. Fan, H.-X. Wang, and S.-K. Li, "Restudy on SVD-based watermarking scheme," *Applied Mathematics and Computation*, vol. 203, no. 2, pp. 926–930, 2008.
- [19] A. A. Mohammad, A. Alhaj, and S. Shaltaf, "An improved SVD based watermarking scheme for protecting rightful ownership," *Signal Processing*, vol. 88, no. 9, pp. 2158–2180, 2008.
- [20] Q. Su, Y. Niu, H. Zou, and X. Liu, "A blind dual color images watermarking based on singular value decomposition," *Applied Mathematics and Computation*, vol. 219, no. 16, pp. 8455–8466, 2013.
- [21] H.-T. Hu and L.-Y. Hsu, "Exploring DWT-SVD-DCT feature parameters for robust multiple watermarking against JPEG and JPEG2000 compression," *Computers and Electrical Engineering*, vol. 41, pp. 52–63, 2015.
- [22] N. M. Makbol and B. E. Khoo, "Robust blind image watermarking scheme based on Redundant Discrete Wavelet Transform and Singular Value Decomposition," *AEU—International Journal of Electronics and Communications*, vol. 67, no. 2, pp. 102–112, 2013.
- [23] N. M. Makbol and B. E. Khoo, "A new robust and secure digital image watermarking scheme based on the integer wavelet transform and singular value decomposition," *Digital Signal Processing*, vol. 33, pp. 134–147, 2014.
- [24] X. Wu and W. Sun, "Robust copyright protection scheme for digital images using overlapping DCT and SVD," *Applied Soft Computing Journal*, vol. 13, no. 2, pp. 1170–1182, 2013.
- [25] P.-P. Zheng, J. Feng, Z. Li, and M.-Q. Zhou, "A novel SVD and LS-SVM combination algorithm for blind watermarking," *Neurocomputing*, vol. 142, pp. 520–528, 2014.
- [26] A. Mishra, C. Agarwal, A. Sharma, and P. Bedi, "Optimized gray-scale image watermarking using DWT-SVD and Firefly Algorithm," *Expert Systems with Applications*, vol. 41, no. 17, pp. 7858–7867, 2014.
- [27] M. Ali and C. W. Ahn, "An optimized watermarking technique based on self-adaptive de in DWT-SVD transform domain," *Signal Processing*, vol. 94, no. 1, pp. 545–556, 2014.
- [28] M. Ali, C. W. Ahn, and M. Pant, "A robust image watermarking technique using SVD and differential evolution in DCT domain," *Optik*, vol. 125, no. 1, pp. 428–434, 2014.
- [29] M. Ali, C. W. Ahn, M. Pant, and P. Siarry, "An image watermarking scheme in wavelet domain with optimized compensation of singular value decomposition via artificial bee colony," *Information Sciences*, vol. 301, pp. 44–60, 2015.
- [30] M. Ali, C. W. Ahn, and P. Siarry, "Differential evolution algorithm for the selection of optimal scaling factors in image watermarking," *Engineering Applications of Artificial Intelligence*, vol. 31, pp. 15–26, 2014.
- [31] S. H. Amiri and M. Jamzad, "Robust watermarking against print and scan attack through efficient modeling algorithm," *Signal Processing: Image Communication*, vol. 29, no. 10, pp. 1181–1196, 2014.
- [32] B. Lei, D. Ni, S. Chen, T. Wang, and F. Zhou, "Optimal image watermarking scheme based on chaotic map and quaternion wavelet transform," *Nonlinear Dynamics*, vol. 78, no. 4, pp. 2897–2907, 2014.
- [33] R.-S. Run, S.-J. Horng, J.-L. Lai, T.-W. Kao, and R.-J. Chen, "An improved SVD-based watermarking technique for copyright protection," *Expert Systems with Applications*, vol. 39, no. 1, pp. 673–689, 2012.
- [34] M. Ali and C. W. Ahn, "Comments on 'optimized gray-scale image watermarking using DWT-SVD and Firefly Algorithm'," *Expert Systems with Applications*, vol. 42, no. 5, pp. 2392–2394, 2015.
- [35] J.-M. Guo and H. Prasetyo, "Security analyses of the watermarking scheme based on redundant discrete wavelet transform and singular value decomposition," *AEU—International Journal of Electronics*
- [36] C.-C. Lai, "An improved SVD-based watermarking scheme using human visual characteristics," *Optics Communications*, vol. 284, no. 4, pp. 938–944, 2011.
- [37] Zheng, Y., Wu, C. H., Lu, Z. M., & Ip, W. H. "Optimal robust image watermarking based on PSO and HVS in integer DCT domain", *International Journal of Computer Sciences and Engineering System*, Vol.2, No.4, pp.281-287, 2008.
- [38] Vahedi, E., Lucas, C., Zoroofi, R. A., & Shiva, M. "A new approach for image watermarking by using particle swarm optimization", In *Proceedings of IEEE ICSPC*, 2007, pp. 1383–1386.
- [39] R. Surya Prakasa Rao, Dr. P. Rajesh Kumar, "An Efficient Genetic Algorithm Based Gray scale Digital Image watermarking for Improving the Robustness and Imperceptibility", In Proc., of International Conference on Electrical, Electronics, and Optimization Techniques (ICEEOT), 2016.
- [40] Hai Tao, Jasni Mohamad Zain, "A wavelet-based particle swarm optimization algorithm for digital image watermarking", *Integrated Computer-Aided Engineering*, Vol.19, pp.81-91, 2012.
- [41] R. Surya Prakasa Rao, Dr. P. Rajesh Kumar, "PSO Based Lossless And Robust Image Watermarking Using Integer Wavelet Transform", *GJCST*, 2016.